iScience

CellPress
OPEN ACCESS

Article

Simple and highly specific targeting of resident microglia with adeno-associated virus

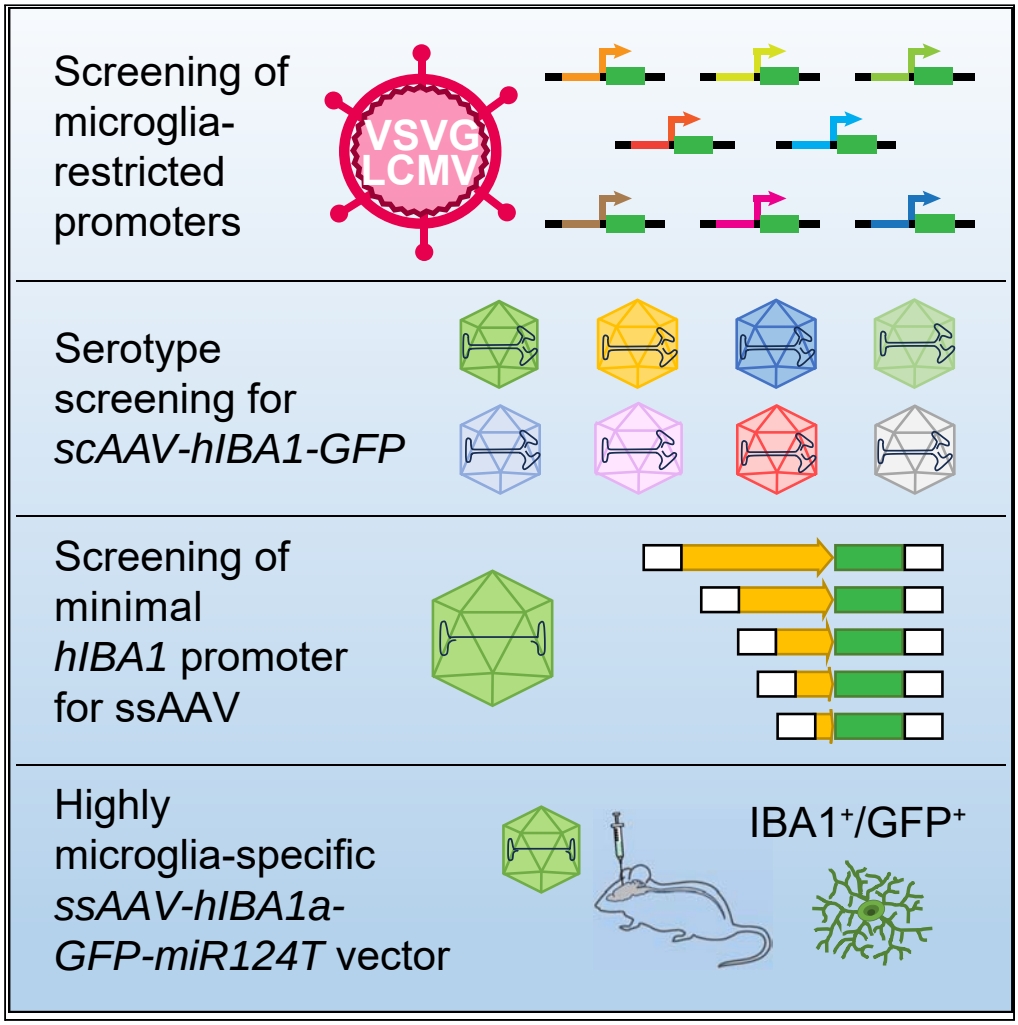

Carolina Serrano, Sergio Cananzi, Tianjin Shen, Lei-Lei Wang, Chun-Li Zhang

chun-li.zhang@utsouthwestern.edu

Highlights

In vivo screening of microglia-targeting lentiviral and AAV vectors

Human *IBA1* promoter (*hIBA1*) drives microglia-restricted gene expression

The 466-bp *hIBA1a* promoter is sufficient to drive microglia-restricted expression

The *ssAAV-hIBA1a-miR124T* vector is highly specific for microglia

Serrano et al., iScience 27, 110706
September 20, 2024
https://doi.org/10.1016/j.isci.2024.110706

iScience

CellPress
OPEN ACCESS

Article

Simple and highly specific targeting of resident microglia with adeno-associated virus

Carolina Serrano,[1,2,4] Sergio Cananzi,[1,2,4] Tianjin Shen,[1,2,4] Lei-Lei Wang,[1,2] and Chun-Li Zhang[1,2,3,5,*]

SUMMARY

Microglia, as the immune cells of the central nervous system (CNS), play dynamic roles in both healthy and diseased conditions. The ability to genetically target microglia using viruses is crucial for understanding their functions and advancing microglia-based treatments. We here show that resident microglia can be simply and specifically targeted using adeno-associated virus (AAV) vectors containing a 466-bp DNA fragment from the human *IBA1* (*hIBA1*) promoter. This targeting approach is applicable to both resting and reactive microglia. When combining the short *hIBA1* promoter with the target sequence of *miR124*, up to 98% of transduced cells are identified as microglia. Such a simple and highly specific microglia-targeting strategy may be further optimized for research and therapeutics.

INTRODUCTION

Microglia serve as the immune cells of the central nervous system (CNS), maintaining homeostasis under normal conditions. They become activated and play dynamic roles during neuroinflammation, neural damage, or under degenerative conditions.[1–6] Depending on the pathological processes, microglia can serve as phagocytes and secrete proinflammatory or anti-inflammatory mediators to regulate degeneration, repair, and regeneration in the CNS.[7] These behaviors of microglia are tightly regulated by extra- and intra-cellular signaling pathways and transcriptional programs.[8,9] Genetic manipulation of microglia will help understand their function as well as hold promising potential for developing new treatments for CNS diseases.

Viral vectors such as lentivirus and adeno-associated virus (AAV) are clinically relevant tools for the genetic manipulation of different cell types.[10–13] Even though lentivirus and AAV can be used to transduce most brain cells, microglia seem to be resistant to the transduction using those vectors.[13–17] The first analysis using AAV2 showed that microglia could be transduced but gene expression was not detectable, suggesting that microglia could have an intrinsic mechanism to prevent transgene expression or virus degradation.[18] The inclusion of microglial specific promoters such as *F4/80* and *CD68* in AAV improved microglia transduction in culture; however, transduction efficiency remained very low in mice.[19] Attempts to improve AAV capsids also failed to induce strong and stable microglia transgene expression.[20]

In this study, we initially aimed to reprogram microglia for neural regeneration, as we have previously done with resident astrocytes and NG2 glia.[21–26] However, multiple attempts failed to efficiently transduce microglia with lentivirus under several routinely used promoters. We therefore conducted *in vivo* screens of additional promoters that could drive gene expression through lentivirus in resident microglia. We mainly focused on human gene promoters with the expectation that such evolutionarily conserved promoters could eventually be used for therapeutics. Based on the results of lentiviruses, we further revealed that a 466-bp fragment of the human *IBA1* (*hIBA1*) promoter, when employed in AAV vectors, was sufficient to drive microglia-specific gene expression. During the process of this study and supporting our results, it was recently reported that a 1.7-kb mouse *Iba1* promoter was also capable of driving microglia-specific expression through AAVs.[27] Notwithstanding, our remarkably short *hIBA1* promoter will allow AAVs to package much larger gene inserts. Although clinically relevant AAV capsids, such as AAV5 and AAV8, can be used to target microglia, our *hIBA1* promoter should be compatible with the recently developed capsid variants for microglia.[28,29]

RESULTS

Specific targeting of microglia with lentivirus under the *hIBA1* promoter

We first examined the lentiviral delivery system to target microglia in the adult mouse brain. We screened eight different promoters associated with specific gene expression in microglia. Except for the mouse *mF4/80* promoter, the remaining seven promoters are human origin, with the aim of targeting human microglia for clinical therapy. They include the *hCD68*, *hIBA1*, *hCX3CR1*, *hC1QA*, *hC1QB*, *hTMEM119*, and *SP* promoters. The reporter *GFP* was put under the control of these promoters, and the lentivirus was packaged with the VSV-G envelope. To

[1]Department of Molecular Biology, University of Texas Southwestern Medical Center, Dallas, TX 75390, USA
[2]Hamon Center for Regenerative Science and Medicine, University of Texas Southwestern Medical Center, Dallas, TX 75390, USA
[3]Peter O'Donnell Jr. Brain Institute, University of Texas Southwestern Medical Center, Dallas, TX 75390, USA
[4]These authors contributed equally
[5]Lead contact
*Correspondence: chun-li.zhang@utsouthwestern.edu
https://doi.org/10.1016/j.isci.2024.110706

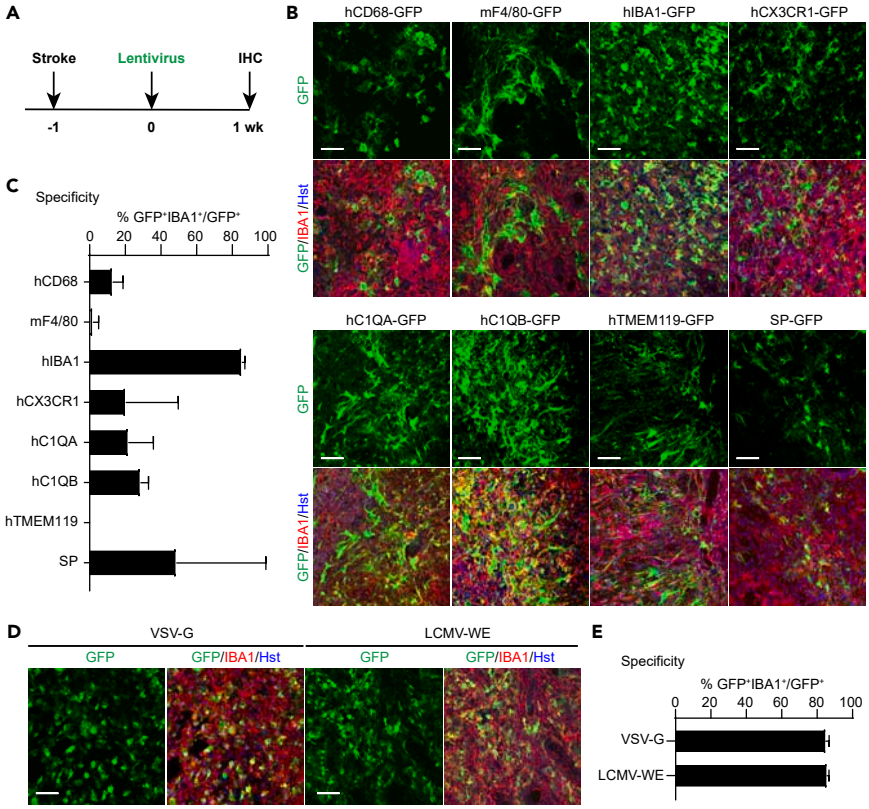

Figure 1. *In vivo* screens for microglia-targeting lentivirus

See also Data S1.

(A) Schematic diagram of the experimental procedure. One week post MCAO-induced stroke, lentiviruses with various promoter-driven GFP were injected into the striata and examined after another week (wk).

(B) Representative confocal images showing marker expression for the indicated lentiviruses. Scale bars, 50 μm.

(C) Quantifications showing high microglia-specificity of GFP expression in mice injected with *lenti-hIBA1-GFP* (mean ± SEM; *n* = 3 mice per group).

(D) Representative confocal images showing marker expression for the indicated lentiviruses. Scale bars, 50 μm.

(E) Quantifications showing comparable specificity of lentivirus packaged with either VSV-G or LCMV-WE envelope (mean ± SEM; *n* = 3 mice per group).

include reactive microglia, which are critically involved in neurological diseases, we induced ischemic stroke through the MCAO procedure one week before virus injections (Figure 1A). One week post virus (wpv) delivery, we analyzed the expression of the reporter GFP expression and the microglia-specific marker IBA1 in the injected mouse striatum. GFP^+IBA1^+ cells were detected in the striatum with all the promoters tested; however, the highest microglia-specific GFP expression was driven by the *hIBA1* promoter (85.64 ± 0.72%; Figures 1B and 1C). GFP driven by the other promoters was detected in both microglia and cells that morphologically appeared to be neurons and astrocytes. Because the best transduction efficiency for microglia was driven by the *hIBA1* promoter, we decided to focus our subsequent studies on this promoter.

Microglia-specific expression is not affected by the lentiviral envelopes

Cell type-specificity of lentiviruses was reported to be influenced by the viral envelopes.[30] To test this possibility, we compared the *hIBA1-GFP* lentivirus packaged with either the VSV-G or the LCMV-WE envelope. When GFP^+IBA1^+ cells were examined at 1 wpv, both enveloped lentiviruses showed high targeting specificity for microglia in the injected striatum (84.96 ± 1.04% for VSV-G and 85.64 ± 0.75% for LCMV-WE; Figures 1D and 1E).

Specific targeting of microglia with self-complementary adeno-associated virus under the *hIBA1* promoter

Lentiviral and AAV vectors are widely applied for gene expression *in vivo*. Even though both systems allow stable transgene expression, AAVs are more broadly employed for *in vivo* gene therapy due to their non-integration nature and minimal inflammatory response.[11,12,31,32] We first examined the self-complementary AAV (scAAV) since it was reported to drive stronger gene expression than the single-stranded AAV (ssAAV).[33] *scAAV-hIBA1-GFP* was then packaged with 8 different capsids, including AAV1, AAV2, AAV5, AAV6, AAV6m, AAV8, AAV9 and PHP.eB. They were injected into the striatum one week post L-NIO-induced stroke (which produces more constant and confined infarcts

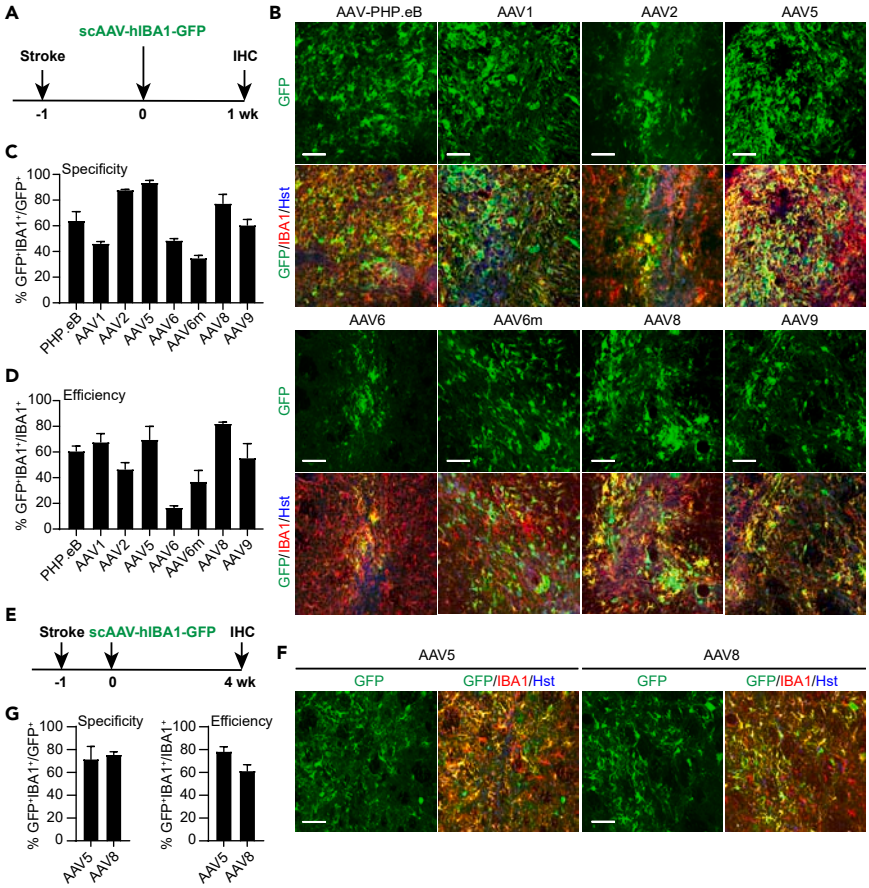

Figure 2. *In vivo* screens for microglia-targeting AAVs

(A) Schematic diagram of the experimental procedure. One week post L-NIO-induced stroke, scAAVs with various capsids were injected into the striata and examined after another week (wk).

(B) Representative confocal images showing marker expression for the indicated scAAVs. Scale bars, 50 μm.

(C) Quantifications showing microglia-specificity of GFP expression for the indicated scAAVs (mean ± SEM; *n* = 3 mice per group).

(D) Quantifications showing microglia transduction efficiency for the indicated scAAVs (mean ± SEM; *n* = 3 mice per group).

(E) Schematic diagram of the experimental procedure. One week post L-NIO-induced stroke, scAAV5 or scAAV8 was injected into the striata and examined after another 4 weeks (wk).

(F) Representative confocal images showing marker expression for the indicated scAAVs. Scale bars, 50 μm.

(G) Quantifications showing the specificity and transduction efficiency for microglia (mean ± SEM; *n* = 3 mice per group).

when compared to the MCAO procedure) and examined 7 days later (Figure 2A). All these scAAVs produced a robust expression of GFP in IBA1$^+$ cells but with varying degrees of specificity and efficiency (Figures 2B–2D). Quantification of GFP$^+$IBA1$^+$ cells showed that both scAAV5 and scAAV8 had the highest degrees of specificity (93.68 ± 1.14% and 77.42 ± 4.97%, respectively; Figure 2C) and efficiency (69.7 ± 7.23% and 82.11 ± 0.8%, respectively; Figure 2D) for microglia.

To determine whether transgene expression could be maintained for longer time *in vivo*, we injected the virus and conducted analysis at 4 wpv (Figure 2E). Both scAAV5 and scAAV8 could mediate robust GFP expression in microglia at this longer delay after virus injection (Figures 2F and 2G). Cell type-specificity and transduction efficiency were comparable to what were observed at 1 wpv.

Identification of the minimal *hIBA1* promoter

The AAV vector has a limited packaging capacity, with about ~4.5 kb for ssAAVs and an even smaller size for scAAV.[34,35] A minimal promoter will help increase the size of the transgene that could be packaged. Our original *hIBA1* promoter is about 760 bp in length, which is already relatively small. To determine whether it could be further shortened, we made a series of truncations starting from the 5′ end and subcloned them into the ssAAV vector. They were then packaged with capsid 5 and injected into the striatum of adult mouse with or without L-NIO-induced stroke (Figures 3A and 3B). When examined at 1 wpv, the 466-bp *hIBA1a* promoter showed a similar expression pattern as the original *hIBA1* promoter, with high microglia specificity and transduction efficiency (70.51 ± 5.12% and 82.26 ± 2.62%, respectively; Figures 3C–3E). Of note, the microglia-specificity was comparable in brains with or without the stroke (70.51 ± 5.15% for sham and 91.93 ± 1.98% for

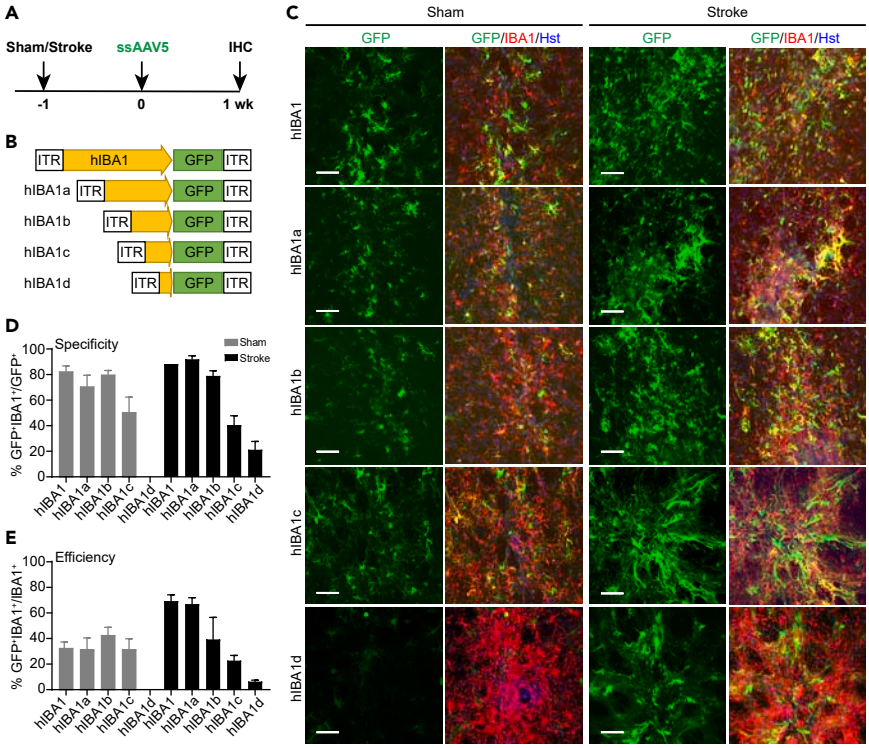

Figure 3. *In vivo* screens for the minimal microglia-targeting promoter

See also Figure S1 and Data S1.

(A) Schematic diagram of the experimental procedure. ssAAV5 viruses with different promoters were injected into sham mice or mice with L-NIO-induced stroke. Brains were analyzed one week later.

(B) Diagram of the examined ssAAVs with different lengths of *hIBA1* promoter.

(C) Representative confocal images showing marker expression for the indicated ssAAV5s. Scale bars, 50 μm.

(D) Quantifications showing microglia-specificity of GFP expression for the indicated ssAAV5s (mean ± SEM; *n* = 3 mice per group).

(E) Quantifications showing microglia transduction efficiency for the indicated ssAAV5s (mean ± SEM; *n* = 3 mice per group).

stroke; Figure 3D), although the transduction efficiency tended to be slightly lower than the non-stroke condition (Figure 3E). The other shorter promoters, especially *hIBA1c* and *hIBA1d*, performed worse. These results suggest that the 466-bp *hIBA1a* promoter could be used for subsequent experiments. When examined at 4 wpv, however, all these viruses showed lower microglia-specificity and transduction efficiency (Figure S1), indicating a time-dependent effect for the ssAAV virus. Future studies are needed to determine the underlying mechanism.

High microglia-specificity of self-complementary adeno-associated virus under the *hIBA1a* promoter

Since the above ssAAVs had dramatically reduced microglia specificity and transduction efficiency at 4 wpv, we then evaluated whether packaging the virus as scAAV would improve the outcome. For this purpose, we prepared the *scAAV5-hIBA1a-GFP* virus, injected it into the striatum of adult mouse with or without L-NIO-induced stroke, and examined gene expression at both 1 and 4 wpv (Figure 4A). We found strong GFP expression in microglia at 1 wpv in both non-injured and injured brains (Figure 4B). The efficiency and specificity for microglia transduction were not only maintained but also slightly increased at 4 wpv, reaching over 80% under the stroke condition (87.62 ± 1.16% for specificity and 88.74 ± 1.12% for efficiency; Figures 4B–4D). These results suggest that the *hIBA1a* promoter could drive highly microglia-specific expression when packaged into scAAV.

miR124T confers high microglia-specificity of self-complementary adeno-associated virus under the *hIBA1a* promoter

Although scAAV can improve the stability of microglia transduction, its limited packaging size could be a problem for larger genes. To maintain microglia specificity but also keep higher packaging capacity, we redesigned a new ssAAV vector under the *hIBA1a* promoter. Since the vast majority of GFP^+ non-microglia cells were neurons, we inserted after the transgene a synthetic sequence containing 4 copies of the targeting sequence of miR124 (Figure 5A, miR124T). miR124 is a microRNA that is highly enriched in neurons.[36] The insertion of miR124T after the transgene is expected to cause silencing of the transgene in neurons but not in other cells.[37] We packaged the *ssAAV5-hIBA1a-GFP-miR124T* virus and injected it into the striatum of mouse without prior injury (Figure 5A). When examined at 4 wpv, we observed robust and highly specific GFP expression in $IBA1^+$ microglia but not in $NeuN^+$ neurons (Figure 5B). Quantification showed that 94.78 ± 0.59% of GFP^+ cells were

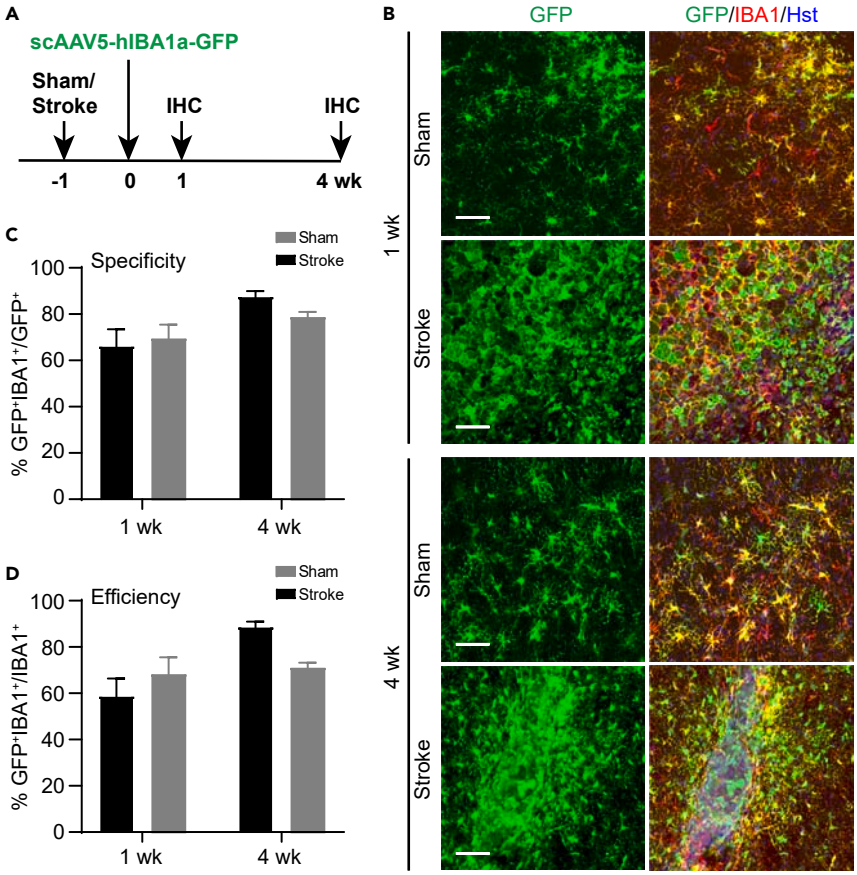

Figure 4. Increased long-term specificity and efficiency for the minimal *hIBA1a* promoter when packaged in scAAV

(A) Schematic diagram of the experimental procedure. scAAV5 virus with the *hIBA1a* promoter was injected into sham mice or mice with L-NIO-induced stroke. Brains were analyzed 1 week or 4 weeks later.

(B) Representative confocal images showing marker expression for the indicated conditions. Scale bars, 50 μm.

(C) Quantifications showing microglia-specificity of GFP expression for the indicated conditions (mean ± SEM; *n* = 3 mice per group).

(D) Quantifications showing microglia transduction efficiency for the indicated conditions (mean ± SEM; *n* = 3 mice per group).

IBA1$^+$ (Figure 5C), indicating a remarkably high microglia-specificity. Transduction efficiency surrounding the injected striatal area was also high, reaching 85.83 ± 1.79% (Figure 5D).

High microglia-specificity in diverse brain regions

To determine whether microglia in other brain regions could also be targeted, we injected a new batch of *ssAAV5-hIBA1a-GFP-miR124T* virus into the hippocampus, striatum, and cortex of adult wild-type mice. Brains were collected for analysis at 4 wpv. GFP expression was largely restricted to IBA1$^+$ cells in these regions, although the GFP$^+$ cells were less dispersed in the cortex compared to those in the striatum and hippocampus (Figures 6A and S2A).

We further examined the hippocampus using additional cell type-specific markers, including PU.1 for microglia, GFAP for astrocytes, NeuN for neurons, and OLIG2 for oligodendrocytes and oligodendrocyte precursor cells (Figure 6B). Quantification showed that GFP was highly specifically detected in microglia both at the injection site (95.56 ± 2.53% for IBA1 and 93.63 ± 0.65% for PU.1) and in regions away from the injection site (98.72 ± 0.74% for IBA1 and 95.58 ± 1.58% for PU.1), while it was not observed in other examined cell types such as astrocytes, neurons, or oligodendrocytes (Figure 6C). The few GFP-positive but IBA1-negative cells, particularly those at the injection sites, might represent a different microglia state commonly observed under pathological conditions.[38] This further suggests that our *hIBA1a* promoter can broadly target microglia, including those with low IBA1 expression. Notably, GFP expression was strong enough for direct imaging without the need for immunostaining (Figure S2B). Additionally, the GFP-expressing area positively correlated with the amount of injected virus (Figure S2C).

DISCUSSION

Our results show that brain microglia can be specifically targeted with AAVs containing a 466-bp *hIBA1* promoter (*hIBA1a*). The microglia specificity is further improved when the target sequence of *miR124* (*miR124T*) is included in the AAV vector to inhibit transgene expression

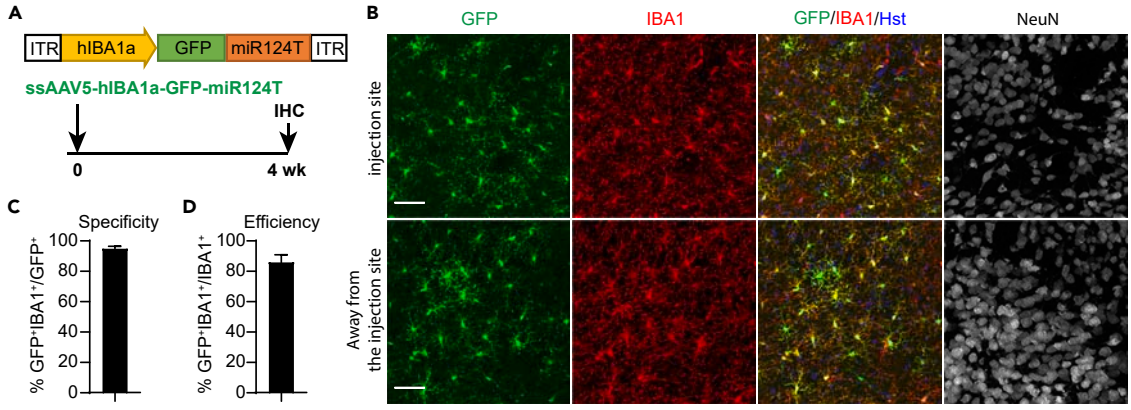

Figure 5. *miR124T* confers high specificity of ssAAV under the *hIBA1a* promoter

(A) Schematic diagram of the experimental procedure. The *miR124T* sequence was inserted into the 3′ end of the *GFP* gene. ssAAV5 virus was then injected into the striatum of adult wild-type mouse and analyzed 4 weeks later.

(B) Representative confocal images showing marker expression in the injection area and an area away from the injection site. Neurons are marked by NeuN staining. Scale bars, 50 μm.

(C) Quantifications showing high microglia-specificity of GFP expression (mean ± SEM; *n* = 3 mice per group).

(D) Quantifications showing high microglia transduction efficiency (mean ± SEM; *n* = 3 mice per group).

in neurons. The *hIBA1a* promoter and *miR124T* could be similarly integrated into lentiviral vectors for lentivirus-mediated targeting of resident microglia.

Although it is well-known that viral tropism is determined by surface proteins in the viral envelope or capsid, cell type-specificity of transgene expression is also controlled by the gene promoters.[12,13,39,40] In lentiviral vectors, our *in vivo* screens showed that the GFP reporter driven by the *hIBA1* promoter exhibited the highest microglia-specificity when compared to any other tested promoters, including the synthetic promoter (*SP*), *hCD68*, *mF4/80*, *hCX3CR1*, *hC1QA*, and *hC1QB*. Future experiments may be needed to tease out the regulatory genomic elements that drive microglia-restricted expression of these latter genes. Of note, the microglia-specificity of lentiviral vectors with the *hIBA1* promoter was not majorly affected by the viral envelope, as we found a comparable specificity for lentivirus packaged with either the VSV-G or the LCMV-WE envelope. Such a result further highlights the importance of the specific promoter for gene expression in microglia.

Because of its low toxicity and minimal induction of host immune responses, AAVs are broadly employed for gene expression *in vivo*.[11,32] Among the many natural capsids of AAVs, AAV1, AAV2, AAV5, AAV6, AAV8, and AAV9 are the most frequently used for research and therapeutics. Our results showed that AAV vectors containing the *hIBA1* promoter, when packaged with any of the above capsids, could drive transgene expression in microglia. Nonetheless, AAV5 and AAV8 gave rise to comparably high transduction specificity and efficiency for microglia. The non-microglia cells for these above tested capsids are mainly neurons and astrocytes, which seem to be the default cell types for the majority AAVs even with a glia-specific promoter.[15,41] To reduce non-specific transgene expression in neurons, we inserted into the AAV vector with 4 copies of the target sequence of *miR124*, a microRNA highly enriched in neurons.[36] Such a strategy greatly improved targeting specificity and long-term expression through AAVs in brain microglia; and it could be similarly employed in lentiviral vectors.

A major limitation of AAVs is their relatively small packaging capacity for foreign DNAs, with roughly 4.5 kb for ssAAVs[34] and an even smaller size for scAAVs.[35] Our systematic truncation analysis showed that a 466-bp genomic fragment of the *hIBA1* promoter is still sufficient to drive microglia-specific gene expression, therefore permitting the insertion of larger genes in both ssAAV and scAAV vectors. Our result is in sharp contrast to a recent report showing a 1.7-kb fragment of the mouse *Iba1* promoter is needed for expression in microglia.[27] Additionally, our short *hIBA1* promoter is expected to work in human microglia; therefore, it should have broader applications than the much longer mouse *Iba1* promoter.

In conclusion, our study identified a straightforward method to specifically target resident microglia using AAVs or lentiviruses. It could be further facilitated with mutant AAV capsids for microglia.[28,29] Our method should be a valuable contribution to microglia-based research and therapeutics.

Limitations of the study

One limitation is the restricted brain distribution of the AAVs when packaged with the capsids we examined. This limitation could be addressed with newly developed mutant AAV capsids[28] or additional mutant capsids obtained through directed molecular evolution. Since the cell type-specificity of AAV-mediated expression could also be influenced by the transgene itself,[41] more genes beyond fluorescence reporters should be examined in the future. Although we examined the stroke condition, it is not known whether cell type-specificity and gene expression levels would differ under other pathological conditions, such as Alzheimer's disease. Additionally, future work is needed to

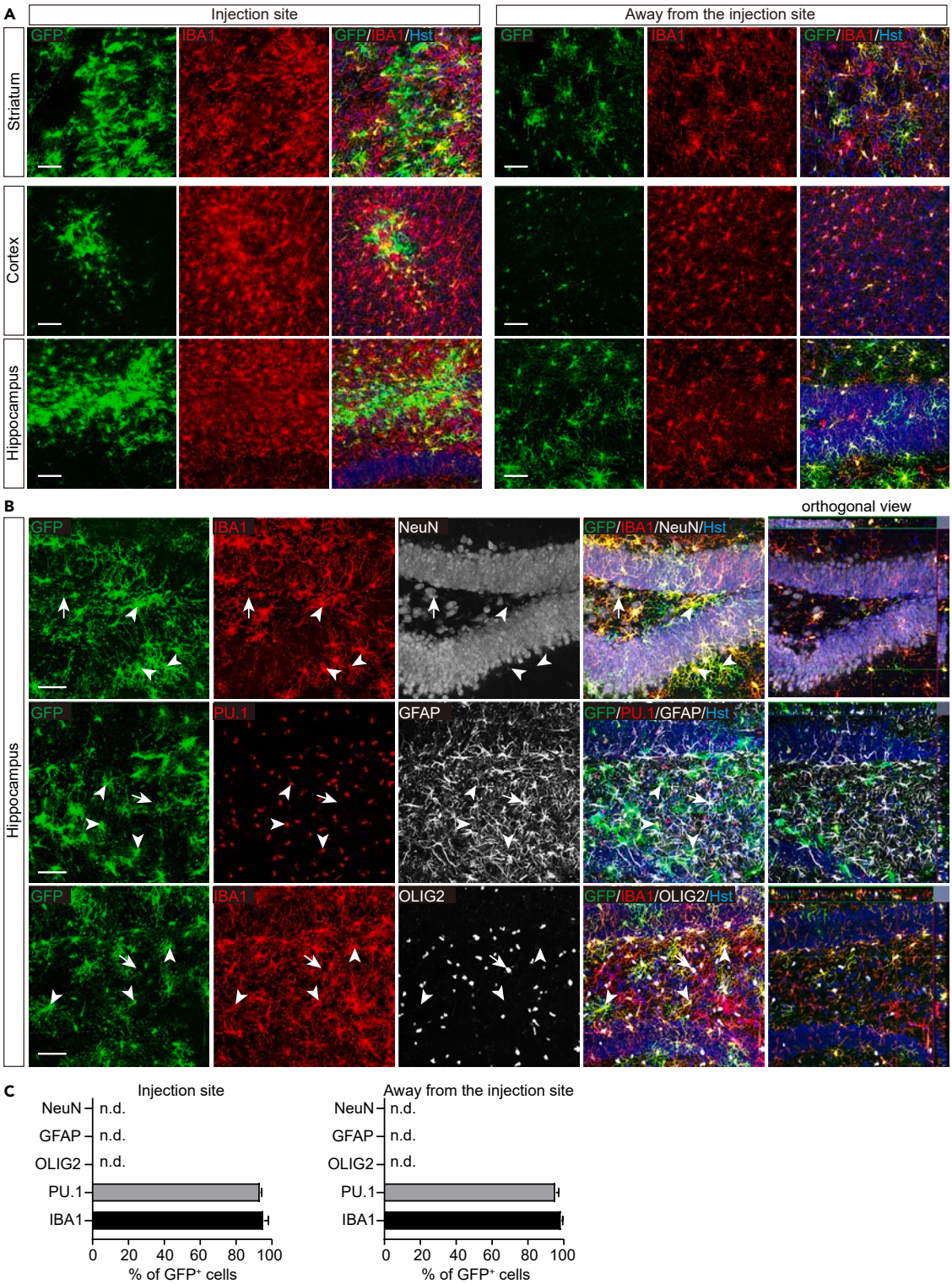

Figure 6. High microglia-specificity in diverse brain regions

See also Figure S2.

(A) Representative confocal images showing marker expression in the injection site and an area away from the injection site. Mouse brains were examined 4 weeks post injection of the *ssAAV5-hIBA1a-GFP-miR124T* virus. GFP signals were from autofluorescence. Scale bars, 50 μm.

Figure 6. *Continued*

(B) Representative confocal images showing marker expression in the hippocampus. GFP signals were from autofluorescence. The arrowheads show examples of GFP^+IBA1^+ or $GFP^+PU.1^+$ microglia, while the arrows indicate GFP are not detectable in $NeuN^+$, $GFAP^+$, or $OLIG2^+$ cells. The orthogonal views are also shown. Scale bars, 50 μm.

(C) Quantifications showing high microglia-specificity of GFP expression in the hippocampus (mean ± SEM; $n = 4$ mice per group; n.d., not detected).

establish a toolbox for AAV-mediated manipulations of microglial activity and function, including vectors for optogenetics, chemogenetics, shRNA-mediated knockdowns, and CRISPR-based applications.

STAR★METHODS

Detailed methods are provided in the online version of this paper and include the following:

- KEY RESOURCES TABLE
- RESOURCE AVAILABILITY
  - Lead contact
  - Materials availability
  - Data and code availability
- METHOD DETAILS
  - Animals
  - Stroke
  - Lentiviral vectors and virus preparation
  - AAV vectors and virus production
  - Stereotactic brain injections
  - Immunohistochemistry and quantifications

SUPPLEMENTAL INFORMATION

Supplemental information can be found online at https://doi.org/10.1016/j.isci.2024.110706.

ACKNOWLEDGMENTS

C.-L.Z. is a W.W. Caruth, Jr. Scholar in Biomedical Research and supported by the Texas Alzheimer's Research and Care Consortium (TARCC), the Decherd Foundation, the Pape Adams Foundation, and NIH grants NS127375, NS117065, and NS111776. We thank members of the C.-L.Z. laboratory for helpful discussions, reagents, and technical assistance, Yuhua Zou for maintaining mouse colonies, Dr. Paramita Chakrabarty at the University of Florida for providing the AAV6 mutant capsid, and Dr. Senlin Li at the University of Texas Health Science Center at San Antonio for providing the lentiviral vector SP–GFP.

AUTHOR CONTRIBUTIONS

C.S., S.C., and T.S. performed experiments, collected data, created figures, and drafted the original article. L.-L.W. provided essential technical support. C.-L.Z. conceived and designed experiments and revised the article. All authors reviewed and approved the final article.

DECLARATION OF INTERESTS

A patent was filed on the use of the *hIBA1* promoter for targeting microglia/macrophages.

Received: March 8, 2024
Revised: June 28, 2024
Accepted: August 7, 2024
Published: August 12, 2024

REFERENCES

1. Colonna, M., and Butovsky, O. (2017). Microglia Function in the Central Nervous System During Health and Neurodegeneration. Annu. Rev. Immunol. *35*, 441–468. https://doi.org/10.1146/annurev-immunol-051116-052358.
2. Kanmogne, M., and Klein, R.S. (2021). Neuroprotective versus Neuroinflammatory Roles of Complement: From Development to Disease. Trends Neurosci. *44*, 97–109. https://doi.org/10.1016/j.tins.2020.10.003.
3. Navarro, V., Sanchez-Mejias, E., Jimenez, S., Muñoz-Castro, C., Sanchez-Varo, R., Davila, J.C., Vizuete, M., Gutierrez, A., and Vitorica, J. (2018). Microglia in Alzheimer's Disease: Activated, Dysfunctional or Degenerative. Front. Aging Neurosci. *10*, 140. https://doi.org/10.3389/fnagi.2018.00140.
4. Wu, Y., Dissing-Olesen, L., MacVicar, B.A., and Stevens, B. (2015). Microglia: Dynamic Mediators of Synapse Development and Plasticity. Trends Immunol. *36*, 605–613. https://doi.org/10.1016/j.it.2015.08.008.
5. Leng, F., and Edison, P. (2021). Neuroinflammation and microglial activation in Alzheimer disease: where do we go from here? Nat. Rev. Neurol. *17*, 157–172. https://doi.org/10.1038/s41582-020-00435-y.

6. Bachiller, S., Jiménez-Ferrer, I., Paulus, A., Yang, Y., Swanberg, M., Deierborg, T., and Boza-Serrano, A. (2018). Microglia in Neurological Diseases: A Road Map to Brain-Disease Dependent-Inflammatory Response. Front. Cell. Neurosci. *12*, 488. https://doi.org/10.3389/fncel.2018.00488.
7. Chen, Y., and Colonna, M. (2022). Two-faced behavior of microglia in Alzheimer's disease. Nat. Neurosci. *25*, 3–4. https://doi.org/10.1038/s41593-021-00963-w.
8. Holtman, I.R., Skola, D., and Glass, C.K. (2017). Transcriptional control of microglia phenotypes in health and disease. J. Clin. Invest. *127*, 3220–3229. https://doi.org/10.1172/JCI90604.
9. Troutman, T.D., Kofman, E., and Glass, C.K. (2021). Exploiting dynamic enhancer landscapes to decode macrophage and microglia phenotypes in health and disease. Mol. Cell *81*, 3888–3903. https://doi.org/10.1016/j.molcel.2021.08.004.
10. Haery, L., Deverman, B.E., Matho, K.S., Cetin, A., Woodard, K., Cepko, C., Guerin, K.I., Rego, M.A., Ersing, I., Bachle, S.M., et al. (2019). Adeno-Associated Virus Technologies and Methods for Targeted Neuronal Manipulation. Front. Neuroanat. *13*, 93. https://doi.org/10.3389/fnana.2019.00093.
11. Haggerty, D.L., Grecco, G.G., Reeves, K.C., and Atwood, B. (2020). Adeno-Associated Viral Vectors in Neuroscience Research. Mol. Ther. Methods Clin. Dev. *17*, 69–82. https://doi.org/10.1016/j.omtm.2019.11.012.
12. Bedbrook, C.N., Deverman, B.E., and Gradinaru, V. (2018). Viral Strategies for Targeting the Central and Peripheral Nervous Systems. Annu. Rev. Neurosci. *41*, 323–348. https://doi.org/10.1146/annurev-neuro-080317-062048.
13. O'Carroll, S.J., Cook, W.H., and Young, D. (2020). AAV Targeting of Glial Cell Types in the Central and Peripheral Nervous System and Relevance to Human Gene Therapy. Front. Mol. Neurosci. *13*, 618020. https://doi.org/10.3389/fnmol.2020.618020.
14. Maes, M.E., Colombo, G., Schulz, R., and Siegert, S. (2019). Targeting microglia with lentivirus and AAV: Recent advances and remaining challenges. Neurosci. Lett. *707*, 134310. https://doi.org/10.1016/j.neulet.2019.134310.
15. Aschauer, D.F., Kreuz, S., and Rumpel, S. (2013). Analysis of transduction efficiency, tropism and axonal transport of AAV serotypes 1, 2, 5, 6, 8 and 9 in the mouse brain. PLoS One *8*, e76310. https://doi.org/10.1371/journal.pone.0076310.
16. Balcaitis, S., Weinstein, J.R., Li, S., Chamberlain, J.S., and Möller, T. (2005). Lentiviral transduction of microglial cells. Glia *50*, 48–55. https://doi.org/10.1002/glia.20146.
17. Wang, S.K., Lapan, S.W., Hong, C.M., Krause, T.B., and Cepko, C.L. (2020). *In Situ* Detection of Adeno-associated Viral Vector Genomes with SABER-FISH. Mol. Ther. Methods Clin. Dev. *19*, 376–386. https://doi.org/10.1016/j.omtm.2020.10.003.
18. Su, W., Kang, J., Sopher, B., Gillespie, J., Aloi, M.S., Odom, G.L., Hopkins, S., Case, A., Wang, D.B., Chamberlain, J.S., and Garden, G.A. (2016). Recombinant adeno-associated viral (rAAV) vectors mediate efficient gene transduction in cultured neonatal and adult microglia. J. Neurochem. *136*, 49–62. https://doi.org/10.1111/jnc.13081.
19. Cucchiarini, M., Ren, X.L., Perides, G., and Terwilliger, E.F. (2003). Selective gene expression in brain microglia mediated via adeno-associated virus type 2 and type 5 vectors. Gene Ther. *10*, 657–667. https://doi.org/10.1038/sj.gt.3301925.
20. Rosario, A.M., Cruz, P.E., Ceballos-Diaz, C., Strickland, M.R., Siemienski, Z., Pardo, M., Schob, K.L., Li, A., Aslanidi, G.V., Srivastava, A., et al. (2016). Microglia-specific targeting by novel capsid-modified AAV6 vectors. Mol. Ther. Methods Clin. Dev. *3*, 16026. https://doi.org/10.1038/mtm.2016.26.
21. Niu, W., Zang, T., Zou, Y., Fang, S., Smith, D.K., Bachoo, R., and Zhang, C.L. (2013). In vivo reprogramming of astrocytes to neuroblasts in the adult brain. Nat. Cell Biol. *15*, 1164–1175. https://doi.org/10.1038/ncb2843.
22. Su, Z., Niu, W., Liu, M.L., Zou, Y., and Zhang, C.L. (2014). In vivo conversion of astrocytes to neurons in the injured adult spinal cord. Nat. Commun. *5*, 3338. https://doi.org/10.1038/ncomms4338.
23. Tai, W., Wu, W., Wang, L.L., Ni, H., Chen, C., Yang, J., Zang, T., Zou, Y., Xu, X.M., and Zhang, C.L. (2021). In vivo reprogramming of NG2 glia enables adult neurogenesis and functional recovery following spinal cord injury. Cell Stem Cell *28*, 923–937.e4. https://doi.org/10.1016/j.stem.2021.02.009.
24. Zhang, Y., Li, B., Cananzi, S., Han, C., Wang, L.L., Zou, Y., Fu, Y.X., Hon, G.C., and Zhang, C.L. (2022). A single factor elicits multilineage reprogramming of astrocytes in the adult mouse striatum. Proc. Natl. Acad. Sci. USA *119*, e2107339119. https://doi.org/10.1073/pnas.2107339119.
25. Tai, W., and Zhang, C.L. (2023). In vivo cell fate reprogramming for spinal cord repair. Curr. Opin. Genet. Dev. *82*, 102090. https://doi.org/10.1016/j.gde.2023.102090.
26. Tai, W., Xu, X.M., and Zhang, C.L. (2020). Regeneration Through *in vivo* Cell Fate Reprogramming for Neural Repair. Front. Cell. Neurosci. *14*, 107. https://doi.org/10.3389/fncel.2020.00107.
27. Okada, Y., Hosoi, N., Matsuzaki, Y., Fukai, Y., Hiraga, A., Nakai, J., Nitta, K., Shinohara, Y., Konno, A., and Hirai, H. (2022). Development of microglia-targeting adeno-associated viral vectors as tools to study microglial behavior in vivo. Commun. Biol. *5*, 1224. https://doi.org/10.1038/s42003-022-04200-3.
28. Young, A., Neumann, B., Segel, M., Chen, C.Z.-Y., Tourlomousis, P., and Franklin, R.J.M. (2023). Targeted evolution of adeno-associated virus capsids for systemic transgene delivery to microglia and tissue-resident macrophages. Proc. Natl. Acad. Sci. USA *120*, e2302997120. https://doi.org/10.1073/pnas.2302997120.
29. Lin, R., Zhou, Y., Yan, T., Wang, R., Li, H., Wu, Z., Zhang, X., Zhou, X., Zhao, F., Zhang, L., et al. (2022). Directed evolution of adeno-associated virus for efficient gene delivery to microglia. Nat. Methods *19*, 976–985. https://doi.org/10.1038/s41592-022-01547-7.
30. Cronin, J., Zhang, X.Y., and Reiser, J. (2005). Altering the tropism of lentiviral vectors through pseudotyping. Curr. Gene Ther. *5*, 387–398. https://doi.org/10.2174/1566523054546224.
31. Li, C., and Samulski, R.J. (2020). Engineering adeno-associated virus vectors for gene therapy. Nat. Rev. Genet. *21*, 255–272. https://doi.org/10.1038/s41576-019-0205-4.
32. Naso, M.F., Tomkowicz, B., Perry, W.L., 3rd, and Strohl, W.R. (2017). Adeno-Associated Virus (AAV) as a Vector for Gene Therapy. BioDrugs *31*, 317–334. https://doi.org/10.1007/s40259-017-0234-5.
33. McCarty, D.M. (2008). Self-complementary AAV vectors; advances and applications. Mol. Ther. *16*, 1648–1656. https://doi.org/10.1038/mt.2008.171.
34. Dong, J.Y., Fan, P.D., and Frizzell, R.A. (1996). Quantitative analysis of the packaging capacity of recombinant adeno-associated virus. Hum. Gene Ther. *7*, 2101–2112. https://doi.org/10.1089/hum.1996.7.17-2101.
35. Wu, J., Zhao, W., Zhong, L., Han, Z., Li, B., Ma, W., Weigel-Kelley, K.A., Warrington, K.H., and Srivastava, A. (2007). Self-complementary recombinant adeno-associated viral vectors: packaging capacity and the role of rep proteins in vector purity. Hum. Gene Ther. *18*, 171–182. https://doi.org/10.1089/hum.2006.088.
36. Smirnova, L., Gräfe, A., Seiler, A., Schumacher, S., Nitsch, R., and Wulczyn, F.G. (2005). Regulation of miRNA expression during neural cell specification. Eur. J. Neurosci. *21*, 1469–1477. https://doi.org/10.1111/j.1460-9568.2005.03978.x.
37. Colin, A., Faideau, M., Dufour, N., Auregan, G., Hassig, R., Andrieu, T., Brouillet, E., Hantraye, P., Bonvento, G., and Déglon, N. (2009). Engineered lentiviral vector targeting astrocytes in vivo. Glia *57*, 667–679. https://doi.org/10.1002/glia.20795.
38. Lier, J., Streit, W.J., and Bechmann, I. (2021). Beyond Activation: Characterizing Microglial Functional Phenotypes. Cells *10*, 2236. https://doi.org/10.3390/cells10092236.
39. Gray, S.J., Foti, S.B., Schwartz, J.W., Bachaboina, L., Taylor-Blake, B., Coleman, J., Ehlers, M.D., Zylka, M.J., McCown, T.J., and Samulski, R.J. (2011). Optimizing promoters for recombinant adeno-associated virus-mediated gene expression in the peripheral and central nervous system using self-complementary vectors. Hum. Gene Ther. *22*, 1143–1153. https://doi.org/10.1089/hum.2010.245.
40. Merienne, N., Le Douce, J., Faivre, E., Déglon, N., and Bonvento, G. (2013). Efficient gene delivery and selective transduction of astrocytes in the mammalian brain using viral vectors. Front. Cell. Neurosci. *7*, 106. https://doi.org/10.3389/fncel.2013.00106.
41. Wang, L.L., Serrano, C., Zhong, X., Ma, S., Zou, Y., and Zhang, C.L. (2021). Revisiting astrocyte to neuron conversion with lineage tracing in vivo. Cell *184*, 5465–5481.e16. https://doi.org/10.1016/j.cell.2021.09.005.
42. He, W., Qiang, M., Ma, W., Valente, A.J., Quinones, M.P., Wang, W., Reddick, R.L., Xiao, Q., Ahuja, S.S., Clark, R.A., et al. (2006). Development of a synthetic promoter for macrophage gene therapy. Hum. Gene Ther. *17*, 949–959. https://doi.org/10.1089/hum.2006.17.949.

STAR★METHODS

KEY RESOURCES TABLE

REAGENT or RESOURCE	SOURCE	IDENTIFIER
Antibodies		
Rabbit polyclonal anti-IBA1	Wako	Cat# 019-19741; RRID: AB_839504
Rabbit monoclonal anti-PU.1 (9G7)	Cell Signaling Technology	Cat# 2258, RRID: AB_2186909
Guinea pig polyclonal anti-NeuN	Synaptic Systems	Cat# 266004; RRID: AB_2619988
Goat polyclonal anti-OLIG2	R&D Systems	Cat# AF2418-SP; RRID: AB_2157554
Chicken polyclonal anti-GFAP	Abcam	Cat# ab4674; RRID: AB_304558
Chick polyclonal anti-GFP	AVES Labs	Cat# GFP-1020; RRID: AB_10000240
Alexa Fluor® 488 AffiniPure Donkey Anti-Chicken IgY (IgG) (H + L)	Jackson Immuno Research Laboratories	Cat# 703-545-155; RRID: AB_2340375
Donkey anti-Rabbit IgG (H + L) Highly Cross Adsorbed Secondary Antibody, Alexa Fluor™ 555	Thermo Fisher Scientific	Cat# A-31572; RRID: AB_162543
Alexa Fluor® 647 AffiniPure F(ab')2 Fragment Donkey Anti-Chicken IgY(IgG) (H + L)	Jackson ImmunoResearch Laboratories	Cat# 703-606-155; RRID: AB_2340380
Alexa Fluor® 647 AffiniPure Donkey Anti-Goat IgG (H + L)	Jackson ImmunoResearch Laboratories	Cat# 705-605-003; RRID: AB_2340436
Goat anti-Guinea Pig IgG (H + L) Highly Cross Adsorbed Secondary Antibody, Alexa Fluor™ 647	Thermo Fisher Scientific	Cat# A-21450; RRID: AB_2535867
Biological samples		
Mouse brain tissue	This paper	N/A
Chemicals, peptides, and recombinant proteins		
L-NIO	Millipore	CAS# 159190–44–0
Nuclease (Benzonase)	Santa Cruz	Cat# sc-202391A
Optiprep density gradient medium	Alere Technologies	Prod. No. 1114542
Polyethylene glycol (PEG)	Sigma	Cat# 81268
Hoechst 33342	Thermo Fisher Scientific	Cat# H3570
Experimental models: organisms/strains		
Mouse: C57BL/6J	The Jackson Laboratory	JAX: 000664; RRID: IMSR_JAX:000664
Oligonucleotides		
ITR forward primer: 5-GGAACCCCTAGTGATGGAGTT-3	Sigma-Aldrich	Customized
ITR reverse primer: 5-CGGCCTCAGTGAGCGA-3	Sigma-Aldrich	Customized
Recombinant DNA		
LV-hCD68-GFP	This paper	N/A
LV-mF4/80-GFP	This paper	N/A
LV-hIBA1-GFP	This paper	N/A
LV-hCX3CR1-GFP	This paper	N/A
LV-hC1QA-GFP	This paper	N/A
LV-hC1QB-GFP	This paper	N/A
LV-hTMEM119-GFP	This paper	N/A

(*Continued on next page*)

Continued

REAGENT or RESOURCE	SOURCE	IDENTIFIER
LV-SP-GFP	Dr. Senlin Li; UT Health Science Center at San Antonio	N/A
scAAV-hIBA1-GFP	This paper	N/A
scAAV-hIBA1a-GFP	This paper; Deposited to Addgene	Cat# 214146; RRID:Addgene_214146
scAAV-hIBA1b-GFP	This paper	N/A
scAAV-hIBA1c-GFP	This paper	N/A
scAAV-hIBA1d-GFP	This paper	N/A
pAAV-hIBA1a-GFP-miR124T	This paper; Deposited to Addgene	Cat# 214147; RRID:Addgene_214147
pAd-deltaF6	Addgene	Cat# 112867; RRID:Addgene_112867
pAAV2/1	Addgene	Cat# 112862; RRID:Addgene_112862
helper pAAV2/2	Addgene	Cat# 104963; RRID:Addgene_104963
helper pAAV2/5	Addgene	Cat# 104964; RRID:Addgene_104964
helper pAAV2/6	Addgene	Cat# 110660; RRID:Addgene_110660
helper pAAV2/6m	Dr. Paramita Chakrabarty at University of Florida	N/A
helper pAAV2/8	Addgene	Cat# 112864; RRID:Addgene_112864
helper pAAV2/9	Addgene	Cat# 112865; RRID:Addgene_112865
pUCmini-iCAP-PHP.eB	Addgene	Cat# 103005; RRID:Addgene_103005
Software and algorithms		
ImageJ	NIH	RRID:SCR_003070, https://imagej.net/Fiji
Graphpad Prism	Graphpad	RRID:SCR_002798), https://www.graphpad.com
ZEN	ZEISS	RRID:SCR_013672, https://www.zeiss.com/microscopy/int/products/microscope-software/zen.html
Adobe Photoshop	Adobe	RRID:SCR_014199, https://www.adobe.com/products/photoshop.html
Adobe Illustrator	Adobe	RRID:SCR_010279, https://www.adobe.com/products/illustrator.html
Other		
stereotaxic apparatus	Stoelting Co., Wood Dale, IL	Cat# 51730
33 gauge, 45-degree-beveled needle	Hamilton, Reno, NV	Cat# 22033 (Customized)
Sliding microtome	Leica	Model SM200R
40-mm nylon strainer	Falcon	Ref. 352340
100K PES concentrator (Pierce)	Thermo Fisher Scientific	Cat# 88524

RESOURCE AVAILABILITY

Lead contact

Further information regarding this manuscript and requests should be directed to the lead contact, Dr. Chun-Li Zhang (chun-li.zhang@utsouthwestern.edu).

Materials availability

The AAV vectors, *scAAV-hIBA1a-GFP* and *pAAV-hIBA1a-GFP-miR124T*, are available from Addgene (#214146 and #214147).

Data and code availability

- Data: All data generated or analyzed during this study are included in the article or its supplemental information.
- Code: This paper does not report original code.
- Any additional information required to reanalyze the data reported in this paper is available from the lead contact upon request.

METHOD DETAILS

Animals

Wild-type C57/BL6J mice were purchased from the Jackson Laboratory. Adult male and female mice at 8 weeks or older were used unless otherwise stated. All mice were housed under a 12 h light/dark cycle and had *ad libitum* access to food and water in the animal facility. Experimental animals were randomized, and the experimenters were not blinded to the allocation of animals during experiments and outcome assessment. All experimental procedures and protocols were approved by the Institutional Animal Care and Use Committee at University of Texas Southwestern.

Stroke

Strokes were induced by either middle cerebral artery occlusion (MCAO) or L-NIO injection. For MCAO, mice were anesthetized with isoflurane. The left common and external carotid arteries were exposed and ligated. Occlusion of the middle cerebral artery (MCA) was accomplished through the insertion of a filament from the basal part of the external carotid artery and advancing it in the internal carotid artery toward the location of MCA branching from the circle of Willis. The occlusion lasted 20 min and reperfusion was initiated by removing the suture from the internal carotid artery. Once the suture was removed, the internal carotid artery was ligated. L-NIO induced ischemia was selected for subsequent experiments because it produced consistent and confined infarcts in the striatum. For L-NIO induced ischemia, a craniotomy was performed overlying the injection sites of the cortex. A Hamilton syringe was filled with L-NIO (27 μg/μL in sterile physiological saline; Calbiochem), secured onto the stereotaxic arm, and connected to a pressure pump. Three injections (each of 0.3 μL of L-NIO solution) were made in the following coordinates: anterior-posterior (AP) +1 mm, medio-lateral (ML) +2 mm, dorsoventral from the skull (DV) −2 mm; AP +1 mm, ML +2 mm, DV −2.5 mm; and AP +1 mm, ML +2 mm, DV −3 mm. Injections were made at a rate of 3 μL/min, targeting the striatum. Localized vasoconstriction leads to focal ischemia in the striatum. In Sham experiments, the needle was placed at the same coordinates as the stroke experiments, but L-NIO was not injected in the striatum.

Lentiviral vectors and virus preparation

The lentiviral vector SP–GFP was generated by sub-cloning the macrophage synthetic promoter (SP, ~400 bp, which harbors multiple myeloid/macrophage cis elements) into the CS–CDF–CG–PRE vector.[42] This SP-GFP vector was a generous gift of Dr. Senlin Li[42] and was used to construct the other lentiviral vectors by replacing the SP at the EcoRI and AgeI sites. The human *CD68* promoter and enhancer (*hCD68*, ~800 bp) was subcloned from *pcDNA3-hCD68prm* (Addgene #34837). The mouse *F4/80* promoter (*mF4/80*, ~670 bp) was PCR-amplified from mouse genomic DNA. The human *IBA1* promoter (*hIBA1*, ~760 bp), human *TMEM119* promoter (*hTMEM119*, ~570 bp), human *CX3CR1* promoter (*hCX3CR1*, ~700 bp), human *C1QA* promoter (*hC1QA*, ~560 bp), and human *C1QB* promoter (*hC1QB*, ~550 bp) were PCR-amplified from human genomic DNA. PCR primers are listed in Data S1. All vectors were verified through restriction enzyme digestions and DNA sequencing. Replication-deficient virus was produced in HEK293T cells by transient transfection with lentiviral vectors and packaging plasmids (pMDL, pREV, and VSV-G or pHCMV-LCMV-WE envelopes). Lentivirus was collected by PEG precipitation and tittered as described previously.[21]

AAV vectors and virus production

The single strand AAV (ssAAV) vectors were based on the *AAV-hGFAP-GFP* vector[41] by replacing the *hGFAP* promoter with the *hIBA1* promoter. The self-complementary AAV (scAAV) vectors were based on the *scAAV-CAG-GFP* vector (Addgene #83279) by replacing the *CAG* promoter with the *hIBA1* promoter. All vectors were verified through restriction enzyme digestions and DNA sequencing. AAV viruses were packaged with *pAd-deltaF6* (Addgene #112867) and one of the following helper plasmids: *pAAV2/1* (Addgene #112862), *pAAV2/2* (Addgene #104963), *pAAV2/5* (Addgene #104964), *pAAV2/6* (Addgene #110660), *pAAV2/6m*,[20] *pAAV2/8* (Addgene #112864), *pAAV2/9* (Addgene #112865), or *pUCmini-iCAP-PHP.eB* (Addgene #103005). Briefly, HEK293T cells were transfected with the packaging plasmids and a vector plasmid. Three days later, virus was collected from the cell lysates and culture media. Virus was purified through iodixanol gradient ultracentrifugation, washed with PBS, and concentrated with 100K PES concentrator (Pierce, Thermo Scientific). Viral titers were determined by quantitative PCR with ITR primers (forward: 5-GGAACCCCTAGTGATGGAGTT-3; reverse: 5-CGGCCTCAGTGAGCGA-3). The complete sequences of the examined *hIBA1* promoter and its truncations are included in Data S1.

Stereotactic brain injections

Viruses were stereotactically injected into the brain of adult mice as described previously.[24] Briefly, mice were placed on a stereotactic frame (Kopf, USA) under isoflurane anesthesia. A vertical skin incision exposed the bregma on the skull used for guiding the location of the Burr hole. Injection coordinates were as follows: AP +1.0 mm, ML ±2.0 mm, and DV -3.0 mm for the striatum; AP +1.0, ML ±1.5, and DV −1.0 for the cortex; AP −2.0, ML ±1.5 to 1.7, and DV −2.0 for the hippocampus. A 10-μL Hamilton syringe with a 33-gauge beveled tip metal needle was used for the injections: 2 μL of lentivirus with an original titer of ~2E+9 cfu/mL, 2 μL of AAV with an original titer of 0.5-8E+13 GC/mL for data presented in Figures 2, 3, 4, and 5, and 1 μL of AAV with an original titer of 1E+12 GC/mL and 1E+13 GC/mL for data presented in Figures 6 and S2. Virus was injected at a rate of 0.5 μL/min until the total volume was delivered. The needle was left in place for 5 min before it was slowly removed from the brain.

Immunohistochemistry and quantifications

Mice were sacrificed and fixed by intracardial perfusion with 4% paraformaldehyde in PBS. Brains were dissected out, post-fixed overnight and cryoprotected with 30% sucrose at 4°C for 48 h. Coronal brain sections were sectioned on a sliding microtome set at 40 μm thickness. The following primary antibodies were used: GFP (GFP-1020, chicken, 1:1,000, Aves Labs), IBA1 (019–19741, rabbit, 1:1,000, Waco), PU.1 (Cat# 2258, rabbit, 1:1,000, Cell Signaling Technology), GFAP (ab4674, chicken, 1:1,000, Abcam), OLIG2 (AF2418-SP, goat, 1:1,000, R&D Systems), and NeuN (266 004, guinea pig, 1:500, Cedarlane-synaptic system). Alexa Fluor 488-, 594- or 647-conjugated corresponding secondary antibodies from Jackson ImmunoResearch were used for indirect fluorescence. Nuclei were counterstained with Hoechst 33342 (Hst). Images were captured and examined by a Zeiss LSM 700 confocal microscope. Three to five random confocal images with marker-positive cells at or surrounding the injection sites were analyzed for each mouse. A total of 200–500 cells were analyzed for each mouse and 3–4 mice were used for each group. Microglia-specificity was calculated as % of $GFP^+IBA1^+/IBA1^+$ cells, whereas viral transduction efficiency was calculated as % of $GFP^+IBA1^+/IBA1^+$ cells surrounding the injection sites.